

X-ray versus Optical Observations of Active Galactic Nuclei: Evidence for Large Grains?

Joseph C. Weingartner & Norman Murray

CITA, 60 St. George Street, University of Toronto, Toronto, ON M5S 3H8, Canada

ABSTRACT

Recently, Maiolino et al. (2001a, A&A, 365, 28) constructed a sample of active galactic nuclei for which both the reddening $E(B-V)$ and the column density N_{H} to the nucleus could be determined. For most of the galaxies in their sample, they found that $E(B-V)/N_{\text{H}}$ is substantially smaller than for the diffuse interstellar medium of our Galaxy. They asserted that either the dust-to-gas ratio is lower than in the Galaxy or that the grains are so large that they do not extinct or redden efficiently in the optical. We show that there is no systematic increase in $E(B-V)$ with N_{H} for the Maiolino et al. (2001a) galaxies, which suggests that the X-ray absorption and optical extinction occur in distinct media.

Maiolino et al. (2001b, A&A, 365, 37) suggested that the observed lines of sight for the Maiolino et al. (2001a) galaxies pass through the “torus” that obscures the broad line region and nuclear continuum in Seyfert 2 galaxies and argued that the torus grains are larger than Galactic grains. There is no reason to believe that the lines of sight for these galaxies pass through the torus, since the observed column densities are lower than those typically observed in Seyfert 2 galaxies. We suggest instead that the X-ray absorption occurs in material located off the torus and/or accretion disk while the optical extinction occurs in material located beyond the torus. The X-ray absorbing material could either be dust-free or could contain large grains that do not extinct efficiently in the optical. There is no conclusive evidence that the grains in active galactic nuclei are systematically larger than those in the diffuse interstellar medium of our Galaxy. We discuss an alternative way to probe the properties of dust in Seyfert tori, but find that observations of Seyfert 2 nuclei with higher resolution than currently available will be needed in order to place stringent limits on the dust.

Subject headings: galaxies: active—galaxies: nuclei—galaxies: ISM—dust, extinction

1. Introduction

The unified model of active galactic nuclei (AGNs) posits that Seyfert 1 (Sy 1) and Seyfert 2 (Sy 2) galaxies are intrinsically the same, but that obscuring matter along our line of sight to the nucleus extincts the broad lines and nuclear continuum in Sy 2s (see Antonucci 1993 for a review).

The obscuring matter is usually referred to as the “torus”, although its geometry has not yet been established.

The torus is located at a distance $r \lesssim 1$ pc from the center, on the basis of the following observational evidence. First, the infrared spectral energy distribution of AGNs is dominated by thermal emission from grains with a range of temperatures extending up to the sublimation temperature, ≈ 1500 – 2000 K. This temperature is reached at a distance $\lesssim 1$ pc from the center. Variations in the IR continuum follow variations in the UV/optical continuum with a delay of \sim hundreds of days, confirming the presence of dust with $r \lesssim 1$ pc. See §4.3 of Peterson (1997) for further details and references. Second, VLBI observations of “megamasers” in AGNs demonstrate that molecules are located at $r \lesssim 1$ pc (see Maloney 2002 for a review).¹ Third, Risaliti, Maiolino, & Salvati (1999) have shown that the column density $N_{\text{H}} \gtrsim 10^{24} \text{ cm}^{-2}$ for at least 50% of Sy 2 galaxies, and have pointed out that if the obscuring matter were located at $r \gtrsim 10$ – 100 pc, then its mass would exceed the dynamical mass for that region.

In addition to Sy 1s and Sy 2s, there are also intermediate-type galaxies, with weaker broad lines than observed in Sy 1s. For example, Sy 1.8 galaxies have very weak broad $\text{H}\alpha$ and $\text{H}\beta$ lines and Sy 1.9s have no detectable broad $\text{H}\beta$. Risaliti et al. (1999) found that the column density (determined from the photoelectric cutoff in the X-ray spectrum) along the line of sight to the nucleus is typically much higher in Sy 2s than in 1.8s and 1.9s (see Figure 1). The lower column densities in intermediate-type Seyferts could possibly result from our line of sight traversing relatively low-density outer regions of the torus. Alternatively, the X-ray-absorbing material in Sy 1.8s and 1.9s might be unrelated to the torus. Maiolino & Rieke (1995) found that Sy 1.8s and 1.9s are mostly found in edge-on host galaxies, implying that the optical extinction is due to dust located beyond the torus. If the optical extinction is unrelated to the torus, then it seems plausible that the same could be true for the X-ray absorption as well.

Maiolino et al. (2001a; hereafter M01a) presented a sample of AGNs for which at least some broad lines are observed, but with significant reddening. For each of the objects in the M01a sample, both the reddening $E(B-V)$ and the total H column density N_{H} along the line of sight to the nucleus have been estimated.² The column density is inferred from observations of the absorption of X-rays from the central source. M01a found that, with the exception of a few low-luminosity AGNs, $E(B-V)/N_{\text{H}}$ is generally lower than it is in the diffuse interstellar medium (ISM) of our Galaxy, by factors of a few up to ~ 100 . M01a assumed that the X-ray-absorbing material and optical-absorbing material are identical, which would imply that either (1) the dust-to-gas ratio in this material is lower than in the Galaxy or (2) the grains in this material are so large that, unlike Galactic grains, they do not extinct and redden efficiently in the optical. In a companion paper, Maiolino, Marconi, & Oliva (2001b; hereafter M01b) argued in favor of the latter

¹The megamaser observations also suggest a warped disk geometry for the torus; see Maloney (2002).

²The reddening is the extinction at B minus the extinction at V ; i.e., $E(B-V) = A_B - A_V$.

interpretation. Their argument assumes that the medium probed by M01a is in fact the torus that is responsible for the optical obscuration of the broad line region (BLR) and nuclear continuum in Sy 2s.

Here, we propose an alternative interpretation, namely, that the lines of sight to the nuclei in the M01a sample pass not through the torus, but through lightly or moderately ionized material located off the torus and/or accretion disk, perhaps in a wind. This material, which is responsible for the X-ray absorption, could be either dust-free or dominated by large enough grains that very little extinction and reddening result. The observed reddening of the BLR occurs in a dusty medium that is physically distinct from the X-ray-absorbing material. In §2 we describe the M01a sample and present evidence that (1) the torus is not being probed and (2) the X-ray- and optical-absorbing gas are distinct. In §3 we review the evidence that led M01b to conclude that the grain size distribution of the obscuring material must be dominated by very large grains, and show that this conclusion does not hold in our alternative scenario. In §4, we discuss a method for determining the extinction per column in Seyfert tori. Currently available observations yield limits that are consistent with the torus dust being similar to Galactic dust, but observations at higher resolution are needed in order to establish more stringent limits. We briefly summarize in §5.

2. The M01a Sample

M01a collected a sample of intermediate AGNs for which both the reddening of the BLR and N_{H} could be estimated from observations. They did not attempt to construct an unbiased sample; an object was included so long as $E(B-V)$ and N_{H} could both be determined and there was no evidence for either “warm” absorption (O VII or O VIII absorption edges) or partial covering of the nucleus. The reddening was found by comparing the ratio of the fluxes in two different broad H recombination lines with the expected intrinsic value. The column density was determined from the photoelectric cutoff in the X-ray spectrum. We reproduce their sample in Table 1; see their Table 1 for further details. Note that many of the objects in the M01a sample are Seyfert 1.8 or 1.9 galaxies.

M01b assumed that the low $E(B-V)/N_{\text{H}}$ found for most of the objects in the sample is a property of the torus, but this is not necessarily true. The bottom panel in Figure 1 shows the column density distribution for the M01a sample. The distribution mirrors the Risaliti et al. (1999) distribution for Sy 1.8s and 1.9s, which may not be obscured by the torus, as discussed in §1. Of course, column densities characteristic of intermediate-type Seyferts are to be expected, since some broad lines are observed in the M01a sample objects.

In Figure 2 we plot $E(B-V)$ versus N_{H} for the M01a galaxies. The three points on the left side of the figure are the three low-luminosity AGNs for which $E(B-V)/N_{\text{H}}$ was found to exceed the Galactic value of $1.7 \times 10^{-22} \text{ mag cm}^2$ (Bohlin, Savage, & Drake 1978). The box is AX J0341-44, for which only an upper limit on $E(B-V)$ has been established.

If the gas that absorbs the X-rays were the same as the gas that absorbs the optical radiation, then we would expect $E(B-V)$ to increase with N_{H} . However, Figure 2 is just a scatter plot, suggesting that the X-ray-absorbing gas and the optical-absorbing gas are, in fact, unrelated. The only hint of a correlation between $E(B-V)$ and N_{H} is the presence of three points in the upper right part of the figure. However, one of these is AX J0341-44 (with just an upper limit on the reddening) and the other two are NGC 1365 and NGC 5506. Both of these latter galaxies are edge-on spirals, and a dust lane is observed to directly cover the nucleus in NGC 1365 (see further discussion below).

Closer examination of some of the well-studied galaxies in the M01a sample yields valuable insight:

Mrk 231. M01a took their X-ray data on Mrk 231 from Turner (1999), who observed it with ROSAT and ASCA. Maloney & Reynolds (2000) have observed it more recently with ASCA, and concluded that the observed X-rays are reflected and that the direct line of sight to the X-ray source is Compton thick ($N_{\text{H}} \gtrsim 10^{24} \text{ cm}^{-2}$).³ Gallagher et al. (2002) observed with Chandra and also concluded that the direct line of sight is Compton thick. R. Maiolino (2002, private communication) has brought our attention to recent (not yet published) XMM-Newton data which suggest that Mrk 231 is Compton thin. We adopt the M01a value for N_{H} in Figure 2, but note that the point representing Mrk 231 should perhaps be located further to the right.

Gallagher et al. (2002) also showed that Mrk 231 is a broad absorption line quasar (BALQSO), since an HST spectrum shows blueshifted C IV absorption. Gallagher et al. interpreted their Chandra observations in the context of the radiatively-driven disk wind model for BALQSOs (Murray et al. 1995). They favor a scenario in which the direct X-rays are absorbed in the highly-ionized “hitchhiking gas”; the observed X-rays are scattered off of the hitchhiking gas and absorbed in the BAL wind (see their Figure 12). If this picture is correct, then the X-ray-absorbing gas is dust-free, since the BAL wind originates well within the dust sublimation radius. We can see this directly from the observed width Δv of the C IV absorption. The sublimation radius $r_{\text{sub}} \sim 0.20 L_{46}^{1/2}$ pc, where L_{46} is the bolometric luminosity in units of $10^{46} \text{ erg s}^{-1}$ (Laor & Draine 1993). If the absorption occurs at r_{sub} , then we expect the width to be $\Delta v_{\text{sub}} \sim (2GM_{\text{BH}}/r_{\text{sub}})^{1/2}$, where M_{BH} is the mass of the black hole. Thus,

$$\Delta v_{\text{sub}} \sim 2.1 \times 10^3 M_8^{1/2} L_{46}^{-1/4} \text{ km s}^{-1} \quad , \quad (1)$$

where M_8 is M_{BH} in units of 10^8 solar masses. The infrared luminosity of Mrk 231 is $\sim 1.5 \times 10^{46} \text{ erg s}^{-1}$ (Rieke & Low 1972, 1975) and, from the Gallagher et al. spectrum, $\Delta v \gtrsim 9 \times 10^3 \text{ km s}^{-1}$. Thus, $\Delta v > \Delta v_{\text{sub}}$, and the BAL wind is within the sublimation radius.

Mrk 231 is also an ultraluminous infrared starburst galaxy and contains ≈ 5 times as much

³Note that O VII and O VIII edges would not be observed in this case, even if these ions were present, since the X-rays are observed in reflection.

molecular gas as the Galaxy (Sanders et al. 1987). Thus, a reddening $E(B-V) \approx 0.34$ due to dust in the host galaxy would not be unexpected.

NGC 1365. Risaliti, Maiolino, & Bassani (2000) observed NGC 1365 with BeppoSAX. Combining their observation with a previous ASCA observation (Iyomoto et al. 1997), Risaliti et al. concluded that there must be a directly observed component and a reflected component. They found that $N_{\text{H}} \approx 4 \times 10^{23} \text{ cm}^{-2}$ for the directly transmitted X-rays and that a Compton-thick component is required near the central source to account for the high reflection efficiency. NGC 1365 is an edge-on spiral galaxy; Edmunds & Pagel (1982) suggested that most of the BLR extinction occurs in a dust lane that has been observed to just barely extend over the nucleus.

IRAS 13197-1627 (= MCG-03-34-064). M01a took broad $\text{H}\alpha$ and $\text{H}\beta$ fluxes from Agüero et al. (1994). However, other authors have reported only narrow lines. Young et al. (1996) concluded that the narrow lines have broad wings and did not find a need for separate broad lines. Thus, this object (with $E(B-V)/N_{\text{H}} \approx 0.0092$ relative to Galactic, the lowest of the M01a AGNs) should be removed from the M01a sample.

NGC 5506. M01a obtained their estimate for the reddening from the ratio of near-infrared lines, taking $\text{Pa}\beta$ from Rix et al. (1990). However, Goodrich, Veilleux, & Hill (1994) argue that there is actually no broad component of the $\text{Pa}\beta$ line, just broad wings on the narrow component. Young et al. (1996) found that the narrow lines are broader in polarized light, supporting the view of Goodrich et al. From the absence of broad $\text{Pa}\beta$, Goodrich et al. conclude that $E(B-V) \gtrsim 3.5$, a factor of 2.2 greater than the reddening adopted by M01a. Given that M01a already found $E(B-V)/N_{\text{H}} = 0.27$ Galactic, the discrepancy between NGC 5506 and the Galaxy is small, if there is any discrepancy at all. Young et al. argue that NGC 5506 is actually a Sy 1 that is heavily reddened by dust in the host galaxy, which is of type S0/a and is seen edge-on (see p. 1242 of their paper for the details of their evidence).

NGC 2992. M01a take the broad line reddening from Gilli et al. (2000). Gilli et al. find the same reddening for the narrow line region (NLR) as for the BLR, and suggest that both are reddened by the same medium, perhaps the dust lane that is observed to run across the nucleus.

MCG-5-23-16. M01a adopt $E(B-V) = 0.6$ from the broad $\text{Pa}\alpha$ and $\text{Br}\gamma$ fluxes measured by Veilleux, Goodrich, & Hill (1997). Veilleux et al. note that it is not clear whether or not broad components of the Balmer lines have been detected. Taking a generous upper limit on the broad $\text{H}\alpha$ flux, they find upper limits on the BLR $E(B-V)$ of 2.3 (1.9) from $\text{Pa}\beta/\text{H}\alpha$ ($\text{Br}\gamma/\text{H}\alpha$). They do not understand the discrepancy with the result derived using only the infrared lines. For the NLR, Durret & Bergeron (1988) found $E(B-V) = 0.85$ from $\text{H}\alpha/\text{H}\beta$ and Goodrich et al. (1994) found $E(B-V) = 0.91$ (0.77) from $\text{H}\alpha/\text{H}\beta$ ($\text{Pa}\beta/\text{H}\alpha$). Ferruit, Wilson, & Mulchaey (2000) imaged MCG-5-23-16 with HST and found a rich dust structure in the vicinity of the nucleus, on the scale of hundreds of pc. They also resolve the NLR, which extends to ≈ 180 pc from the nucleus in two opposite directions. Based on color variations across their images, they tentatively find $E(B-V) \approx 0.8$ for the nucleus, consistent with the above determinations for the NLR. If the

BLR $E(B-V) = 0.6$, then it appears that the reddening is due to dust located in the host galaxy, well beyond the torus. If the BLR $E(B-V) \gtrsim 2$, then this may still be the case, but it could also be that some of the reddening arises in material much closer to the nucleus.

IRAS 05189-2524. M01a take the reddening from Severgnini et al. (2001), who found $E(B-V) = 0.7$ for the BLR from $\text{Pa}\alpha/\text{Pa}\beta$. Severgnini et al. also report the fluxes in the narrow lines, and their ratio yields a NLR reddening that is a factor of 2.8 times *larger* than the BLR reddening. If this is correct, then it certainly suggests that dust in the host galaxy is responsible. However, Veilleux, Sanders, & Kim (1999), who also measured broad $\text{Pa}\alpha$ and $\text{Pa}\beta$, caution against using $\text{Pa}\beta$ to determine the reddening, because its profile is affected by strong absorption features arising in Earth’s atmosphere. Veilleux et al. (1999) find $E(B-V) \gtrsim 2.8$ for the BLR from $\text{Pa}\alpha$ and the upper limit on $\text{H}\alpha$ from Veilleux et al. (1997). Veilleux et al. (1999) find $E(B-V) = 2.6$ (2.0) for the NLR from $\text{Pa}\beta/\text{H}\alpha$ ($\text{H}\alpha/\text{H}\beta$).

NGC 526a. Winkler (1992) found that the NLR is unreddened and did not detect broad lines. Winkler mentions that an unpublished spectrum taken by Martin Ward in 1978 did detect broad $\text{H}\alpha$ and $\text{H}\beta$, and that the line ratio indicated substantial reddening. Thus, this object might be a case in which the BLR-obscuring dust is located in the vicinity of the torus. M01a cite Marconi et al. (in preparation) for the reddening; this paper apparently has not yet been published.

To summarize this section, a plot of $E(B-V)$ versus N_{H} for the M01a sample suggests that the X-ray absorption and optical extinction arise in different material. Observations of several of the M01a galaxies reveal that the optical extinction arises at $r \gtrsim 100$ pc, beyond the location of the torus. This is consistent with the following two results: (1) most Sy 1.8s and 1.9s are located in edge-on galaxies (Maiolino & Rieke 1995) and (2) the nuclear reddening in Sy 1s increases with the inclination angle of the host galaxy (Crenshaw & Kraemer 2001 and references therein). In a couple of cases, there are also indications that the X-ray-absorbing gas is located close to the center, at $r \lesssim 1$ pc. Finally, the low inferred column densities suggest that the line of sight does not pass through the torus, or at most only through a relatively low density outer layer of the torus. Taken together, these pieces of evidence strongly contradict the M01a and M01b interpretation that $E(B-V)/N_{\text{H}}$ is substantially lower than Galactic for AGN tori. Rather, the evidence suggests that the M01a AGNs suffer optical extinction farther out in the host galaxy (on scales of ~ 0.1 – 1 kpc) and X-ray absorption in close to the nucleus, in material that lacks typical Galactic grains, and that the obscuring torus is not being probed in these objects.

3. Large Grains?

M01b considered various possible explanations for the low $E(B-V)/N_{\text{H}}$ found in the M01a sample and dismissed most of them. For example, they considered the possibility that the broad lines are not viewed directly through the same material that absorbs the X-rays, but rather are seen in reflection from a medium located at some distance from the center, with a lower column

of material between us and the scattering medium. However, the observed polarization of the broad lines is usually much lower than would be expected in this case. Furthermore, the generally low scattering efficiency would imply unexpectedly large intrinsic broad line intensities, given the observed fluxes.

M01b also considered the possibility that the line of sight to the central X-ray source encounters different material than the line of sight to the BLR. Although this could certainly occur, it is unlikely to be the case for all of the galaxies discussed by M01a, since the distance from the center to the BLR is much less than the distance to the torus.

Perhaps the most obvious explanation is that the dust-to-gas ratio in the obscuring material is lower than it is in the Galaxy. M01b argue that this cannot be the case for all of the M01a galaxies as follows. As mentioned above, they assume that the obscuring medium is the torus, which presumably consists largely of neutral gas. Thus, most of the H-ionizing ultraviolet photons will be absorbed, either by dust or by gas. In the latter case, emission in H recombination lines results. If the torus has a covering factor of $\sim 80\%$ (see below for further discussion of this), then in the dust-depleted case a large fraction of the ultraviolet continuum will be reprocessed into H recombination lines, with widths comparable to the narrow line widths. On the other hand, the narrow line intensities imply a NLR covering factor of $\sim 8\%$. Thus, the dust depletion scenario would lead to ~ 10 times too much narrow line emission.

M01b argued that this problem can be avoided if the dust is dominated by large grains. The grains are large enough that the extinction efficiency is low in the optical, yielding the low $E(B-V)/N_H$, yet are still able to absorb enough of the UV continuum to suppress the H recombination lines.

As discussed in §2, the torus most likely does not lie along our line of sight to the nucleus for the M01a galaxies. We agree with M01b that ionizing photons incident on the torus are absorbed by grains, but in our scenario these grains need not be different from Galactic grains. We can estimate the covering factor of the X-ray-absorbing material probed by the M01a sample from the fraction of Seyferts that are of intermediate type. Maiolino & Rieke (1995) found that the ratio Sy 2 : Sy (1.8+1.9) : Sy (1+1.2+1.5) $\approx 3:1:1$ and concluded that the intermediate Seyferts usually are obscured not by the torus proper, but by material in the host galaxy located at a greater distance from the nucleus. This led M01b to take the covering factor of neutral material to be 80%. We conclude that the covering factor of the X-ray-absorbing material probed by the M01a sample is as low as 20% (if it does not overlap the torus) and as high as 80% (if it also covers the 60% of the sky covered by the torus). In any case, the effective covering factor is 20%, since any line emission originating from behind the torus would not be visible. Thus, if this material were neutral and dust-free, then the excess H recombination line intensity is reduced from a factor of ~ 10 to a factor of ~ 2.5 .

However, the H in this material is probably ionized. For dust-free gas, the largest possible

ionized column density can be found by balancing ionization and recombination:

$$N_{\text{H}} \approx 6 \times 10^{23} \text{ cm}^{-2} \left(\frac{\dot{N}}{10^{54} \text{ s}^{-1}} \frac{10^{-13} \text{ cm}^3 \text{ s}^{-1}}{\alpha_r} \frac{n}{10^5 \text{ cm}^{-3}} \right)^{1/3}, \quad (2)$$

where \dot{N} is the rate at which H-ionizing photons are emitted from the central source and α_r is the case B radiative recombination coefficient. We estimate $\dot{N} \sim 10^{54} \text{ s}^{-1}$ by taking an ionizing luminosity of $10^{44} \text{ erg s}^{-1}$ and an average photon energy of 50 eV. For $T = 10^4 \text{ K}$ (10^5 K), $\alpha_r = 4.2 \times 10^{-13}$ ($6.9 \times 10^{-14} \text{ cm}^3 \text{ s}^{-1}$).⁴ Thus, we expect that the central source can typically maintain an ionized column density of $N_{\text{H}} \approx 6 \times 10^{23} \text{ cm}^{-2}$, which is a factor ≈ 2 larger than the highest N_{H} in the M01a sample (for IRAS 13197-1627, which, as we showed in §2, should be removed from the M01a sample, or NGC 1365). In other words, for NGC 1365, only half of the ionizing photons are absorbed by the gas, assuming it is dust-free. The other half could either be absorbed by dust farther out in the host galaxy or escape the host galaxy altogether. Since significant reddening is observed for the M01a galaxies, the former alternative is generally more likely. In either case, only half of the ionizing photons passing through this medium result in H recombination lines. Thus, for NGC 1365, the excess narrow line power is reduced from a factor 2.5 to a factor 1.25. For the other galaxies in the M01a sample, with lower N_{H} , a smaller (often much smaller) fraction of the ionizing photons are absorbed, and there is no excess narrow line power. Thus, in our scenario there is no need for larger-than-Galactic grains in active galactic nuclei. They are not needed in the torus, since the M01a observations do not probe the torus and hence do not rule out Galactic-type grains. They are not needed in the material probed by the M01a sample, because this material is ionized and has a lower covering factor than the torus.

M01a pointed out two other observations that they claim argue against the presence of typical Galactic grains in the obscuring media in AGNs. First, the 2175 Å extinction feature, which is nearly ubiquitous in the Galaxy and is usually attributed to carbonaceous grains, has not been observed in those Sy 1s for which some extinction has been measured. Li & Draine (2001) and Weingartner & Draine (2001) suggested that the 2175 Å feature is due to polycyclic aromatic hydrocarbon (PAH) molecules. PAHs can be destroyed in the harsh radiation environment of AGNs (see, e.g., Voit 1992), so the absence of the 2175 Å feature in Sy 1s is perhaps not surprising. It is interesting to note that the 2175 Å feature is also absent in the SMC bar (Gordon & Clayton 1998). In intermediate and type 2 Seyferts, the extinction is so strong that the UV emission is completely suppressed, and there is no chance to search for the 2175 Å feature. Since the extinction in Sy 1s is not due to the torus, the lack of the 2175 Å feature in these objects does not tell us about the dust in the torus.

M01a also noted that the 9.7 μm feature (associated with silicate grains with sizes $\lesssim 3 \mu\text{m}$) is generally very weak in AGNs. Clavel et al. (2000) found that this feature appears weakly in

⁴We evaluate α_r using the FORTRAN routine *rrfit*, written by D. A. Verner, and available at <http://www.pa.uky.edu/~verner/fortran.html>.

emission in Sy 1s and may appear in either emission or absorption in Sy 2s, in either case very weakly. It is difficult to determine the silicate feature accurately because of strong PAH emission features on either side of it. Clavel et al. inferred that there is substantial mid-infrared extinction in Sy 2s; M01a concluded that there must therefore be grains in the torus, but that they must be large enough to not produce a $9.7\mu\text{m}$ absorption feature. We consider this to be the best piece of evidence for large grains in Seyfert tori. Unlike the M01a sample, the Clavel et al. observations apparently do probe the torus. M01a noted that radiative transfer effects could possibly lead to the weak silicate feature in Sy 2s, but considered this unlikely. In this context, it is interesting to note that earlier observations (that did not take into account the PAH absorption near $9.7\mu\text{m}$) found the $9.7\mu\text{m}$ feature to be absent in Sy 1s but strongly present in absorption in Sy 2s (Roche et al. 1991). Although this was initially perplexing, Manske et al. (1998) were able to find a simple radiative transfer scheme that could account for the observations. Further study is needed to determine whether the Clavel et al. observations can be explained by a radiative transfer scheme when silicate grains with $a \lesssim 3\mu\text{m}$ are present.

4. Extinction in Sy 2s

As discussed above, the study of reddening in intermediate-type Seyferts probably does not inform us about the properties of grains in the obscuring torus. Perhaps an analysis of extinction in Sy 2s could be helpful. Narrow-aperture observations of the nucleus (e.g., in the optical or near-infrared) would yield fluxes which can be compared with the flux expected in the case of no obscuration, using an isotropic indicator of the intrinsic luminosity (e.g., [O III] $\lambda 5007$; see Bassani et al. 1999). This would yield a lower limit on the extinction due to the torus, since some of the observed flux could be due to scattering of the nuclear radiation and/or to emission by material located beyond the torus.

Quillen et al. (2001) compiled high-resolution HST images of Seyfert galaxies at $1.6\mu\text{m}$ and tabulated the nuclear fluxes at this wavelength. In this section, we use their data to try to constrain $A_{1.6}/N_{\text{H}}$ for Seyfert tori ($A_{1.6}$ is the extinction at $1.6\mu\text{m}$). Note that $1.6\mu\text{m}$ is approximately the shortest wavelength at which emission from hot dust can be observed; if the dust were hot enough to emit at shorter wavelengths, then it would have sublimated away. Thus, observations at somewhat shorter wavelengths, if available, would be preferable.

In Table 2 we list $1.6\mu\text{m}$ fluxes for all of the Sy 1+1.2+1.5 galaxies from Quillen et al. for which [O III] fluxes are available from Whittle (1992). In Figure 3 we plot the $1.6\mu\text{m}$ luminosities versus the [O III] luminosities for these galaxies (squares; cf Figure 3a in Quillen et al.). We infer the distances to the galaxies from the radial velocities, assuming the Hubble constant $H = 60 \text{ km s}^{-1} \text{ Mpc}^{-1}$. A least squares fit yields the expected intrinsic $1.6\mu\text{m}$ luminosity $L_{1.6}^{\text{int}}$ as a function of the observed [O III] luminosity L_{O} : $L_{1.6}^{\text{int}} = 2.83 \times 10^{11} L_{\text{O}}^{0.766}$ (with the luminosities in erg s^{-1}). Note the large scatter of the observations about the fit, due in part to the large uncertainties in the [O III] fluxes (Whittle 1992).

In Table 3 we list the Sy 2 galaxies from Quillen et al. for which [O III] fluxes and N_{H} (measurements or lower limits) are available from Bassani et al. (1999) or Risaliti et al. (1999). We also include these Sy 2s in Figure 3; note that they mostly lie well below the Sy 1s. We estimate $A_{1.6}$ by comparing the observed $1.6\mu\text{m}$ luminosity, $L_{1.6}^{\text{obs}}$, with $L_{1.6}^{\text{int}}$ and compare $A_{1.6}/N_{\text{H}}$ with the typical value for the diffuse ISM in our Galaxy, $1.0 \times 10^{-22} \text{ cm}^2$ (Cardelli, Clayton, & Mathis 1989); see Table 3. In cases where only an upper limit on the $1.6\mu\text{m}$ flux was established, a lower limit on $A_{1.6}/N_{\text{H}}$ results. Similarly, upper limits on $A_{1.6}/N_{\text{H}}$ are established when only lower limits on N_{H} are available.

The resulting $A_{1.6}/N_{\text{H}}$ (normalized to the typical Galactic value) cover a range similar to the Galactic-normalized $E(B-V)/N_{\text{H}}$ found by M01a for intermediate Seyferts. We suspect that the large values obtained for NGC 1672 and NGC 3079 may be due to underestimates of N_{H} . In Figure 4, we plot $A_{1.6}$ versus N_{H} . As for the M01a sample, $A_{1.6}$ does not systematically increase with N_{H} , indicating that we have not actually determined $A_{1.6}/N_{\text{H}}$ for the torus. For most of the objects, $L_{1.6}^{\text{obs}} \lesssim 0.1 L_{1.6}^{\text{int}}$ (i.e., $A_{1.6} \gtrsim 2.5$). Since the HST resolution at the distances of the observed galaxies is $\gtrsim 10 \text{ pc}$, scattering at locations beyond the torus could be responsible for most of the observed $1.6\mu\text{m}$ flux. In other words, the determinations of $A_{1.6}/N_{\text{H}}$ in this section should actually be interpreted as lower limits. The large scatter of the Sy 1 galaxies about the $L_{1.6}$ – L_{O} relation indicates that inferred values of $A_{1.6} \lesssim 2$ are suspect. Also, galaxies with low inferred $A_{1.6}$ might have an unresolved star cluster very close to the nucleus (Quillen et al. 2001). Thus, the results in this section are entirely consistent with the dust in Seyfert tori being similar to Galactic dust. More stringent limits on the extinction per column will require higher resolution. Improved measurements of [O III] fluxes (for both Sy 1s and 2s) would also be helpful.

5. Summary

M01a constructed a sample of intermediate-type Seyfert galaxies that have been observed in the X-ray and in the optical or infrared and found that $E(B-V)/N_{\text{H}}$ is substantially lower than its value in the Galaxy for most of the objects in the sample. M01b concluded that the only viable explanation for this result is that the grains in Seyfert tori are typically substantially larger than the grains in the ISM of our Galaxy.

Here, we have shown that the material that absorbs the X-rays is probably unrelated to the material that absorbs the optical/infrared radiation (§2, Figure 2) and that the torus probably is not probed by the observations of the M01a sample (§2, Figure 1). We suggest that, alternatively, the line of sight towards an M01a galaxy passes through ionized material located just off the torus and/or the accretion disk. This material is responsible for the X-ray absorption, while the optical/infrared extinction occurs in material farther from the nucleus, where the dust may be quite similar to Galactic dust. The X-ray-absorbing material may be dust-free or may contain large grains that have very small extinction efficiencies in the optical/infrared (§3). This material may be associated with a disk wind, which would originate within the dust sublimation radius.

In this case, the material would naturally be dust-free. The disk wind scenario can be tested by searching for blue-shifted absorption by ions characteristic of lightly or moderately ionized gas, e.g., C IV. However, such ultraviolet absorption lines could be difficult to detect due to the moderate levels of extinction.

Although the M01a sample does not present evidence in favor of large grains in AGN tori, nor does it present evidence against large grains. The apparent lack of strong $9.7\mu\text{m}$ silicate absorption in Sy 2s could indicate large grains in Seyfert tori, as pointed out by M01a. More detailed studies of radiative transfer are needed in order to clarify this point.

We have attempted to obtain limits on the $1.6\mu\text{m}$ extinction per column in Sy 2s (§4), but the HST does not have adequate resolution to exclude nuclear light that is scattered into our line of sight from locations beyond the torus. Current observations are consistent with the torus dust being similar to Galactic dust; observations at higher resolutions will yield more stringent limits.

We are grateful to R. W. Goodrich, R. Maiolino, and A. C. Quillen for helpful discussions. This research was supported by NSERC of Canada and has made use of the SIMBAD database, operated at CDS, Strasbourg, France and the NASA/IPAC Extragalactic Database (NED) which is operated by the Jet Propulsion Laboratory, California Institute of Technology, under contract with the National Aeronautics and Space Administration.

REFERENCES

- [Agüero, E. L., Calderón, J. H., Paolantonio, S., & Suárez Boedo, E. 1994, PASP, 106, 978
- [Antonucci, R. 1993, ARA&A, 31, 473
- [Bassani, L., Dadina, M., Maiolino, R., Salvati, M., Risaliti, G., Della Ceca, R., Matt, G., & Zamorani, G. 1999, ApJS, 121, 473
- [Bohlin, R. C., Savage, B. D., & Drake, J. F. 1978, ApJ, 224, 132
- [Cardelli, J. A., Clayton, G. C., & Mathis, J. S. 1989, ApJ, 345, 245
- [Cecil, G., Wilson, A. S., & Tully, R. B. 1992, ApJ, 390, 365
- [Crenshaw, D. M. & Kramer, S. B. 2001, ApJ, 562, L29
- [Dickey, J. M. & Lockman, F. J. 1990, ARA&A, 28, 215
- [Durret, F. & Bergeron, J. 1988, A&AS, 75, 273
- [Edmunds, M. G. & Pagel, B. E. J. 1982, MNRAS, 198, 1089
- [Ferruit, P., Wilson, A. S., & Mulchaey, J. 2000, ApJS, 128, 139

- Gallagher, S. C., Brandt, W. N., Chartas, G., Garmire, G. P., & Sambruna, R. M. 2002, *ApJ*, 569, 655
- Gilli, R., Maiolino, R., Marconi, A., Risaliti, G., Dadina, M., Weaver, K. A., & Colbert, E. J. M. 2000, *A&A*, 355, 485
- Goodrich, R. W., Veilleux, S., & Hill, G. J. 1994, *ApJ*, 422, 521
- Gordon, K. D. & Clayton, G. C. 1998, *ApJ*, 500, 816
- Iyomoto, N. et al. 1997, *PASJ*, 48, 425
- Landi, R., et al. 2001, *A&A*, 379, 46
- Laor, A. & Draine, B. T. 1993, *ApJ*, 402, 441
- Li, A. & Draine, B. T. 2001, *ApJ*, 554, 778
- Maiolino, R., Marconi, A., Salvati, M., Risaliti, G., Severgnini, P., Oliva, E., La Franca, F., & Vanzì, L. 2001a, *A&A*, 365, 28 (M01a)
- Maiolino, R., et al. 2000, *A&A*, 355, L47
- Maiolino, R., Marconi, A., & Oliva, E. 2001, *A&A*, 365, 37 (M01b)
- Maiolino, R. & Rieke, G. H. 1995, *ApJ*, 454, 95
- Maloney, P. R. 2002, *astro-ph/0203496*
- Maloney, P. R. & Reynolds, C. S. 2000, *ApJ*, 545, L23
- Manske, V., Henning, Th., & Men’shchikov, A. B. 1998, *A&A*, 331, 52
- Murray, N., Chiang, J., Grossman, S. A., & Voit, G. M. 1995, *ApJ*, 451, 498
- Peterson, B. M. 1997, *An Introduction to Active Galactic Nuclei* (Cambridge: Cambridge University Press)
- Quillen, A. C., McDonald, C., Alonso-Herrero, A., Lee, A., Shaked, S., Rieke, M. J., & Rieke, G. H. 2001, *ApJ*, 547, 129
- Rieke, G. H. & Low, F. J. 1972, *ApJ*, 176, L95
- Rieke, G. H. & Low, F. J. 1975, *ApJ*, 200, L67
- Risaliti G., Maiolino, R., & Salvati, M. 1999, *ApJ*, 522, 157
- Risaliti G., Maiolino, R., & Bassani, L. 2000, *A&A*, 356, 33
- Rix, H.-W., Rieke, G., Rieke, M., & Carleton, N. P. 1990, *ApJ*, 363, 480

- [Roche, P. F., Aitken, D. K., Smith, C. H., & Ward, M. J. 1991, MNRAS, 248, 606
- [Sanders, D. B., Young, J. S., Scoville, N. Z., Soifer, B. T., & Danielson, G. E. 1987, ApJ, 312, L5
- [Severgnini, P., Risaliti, G., Marconi, A., Maiolino, R., & Salvati, M. 2001, A&A, 368, 44
- [Turner, T. J. 1999, ApJ, 511, 142
- [Veilleux, S., Goodrich, R. W., & Hill, G. J. 1997, ApJ, 477, 631
- [Veilleux, S., Sanders, D. B., & Kim, D.-C. 1999, ApJ, 522, 139
- [Voit, G. M. 1992, MNRAS, 258, 841
- [Weingartner, J. C. & Draine, B. T. 2001, ApJ, 548, 296
- [Whittle, M. 1992, ApJS, 79, 49
- [Winkler H. 1992, MNRAS, 257, 677
- [Young, S., Hough, J. H., Efstathiou, A., Wills, B. J., Bailey, J. A., Ward, M. J., & Axon, D. J. 1996, MNRAS, 281, 1206

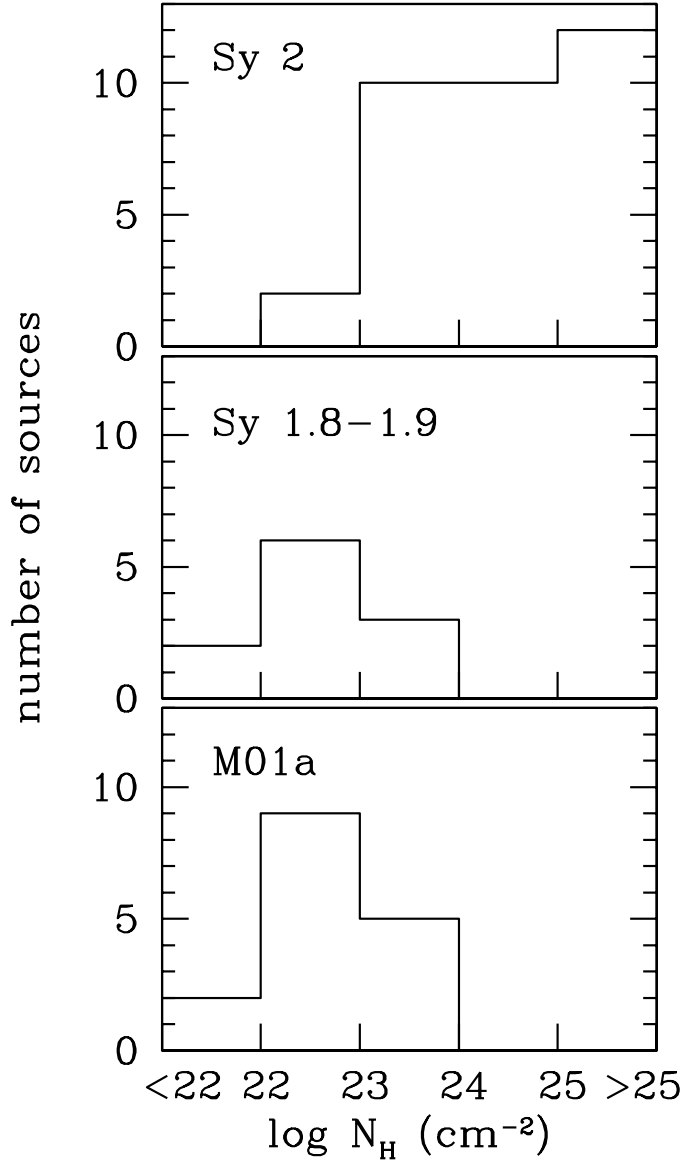


Fig. 1.— X-ray-absorbing column density (N_{H}) distribution for Sy 2 and intermediate Sy (1.8–1.9) galaxies in the “optimal” sample of Risaliti et al. (1999) and for the galaxies in the M01a sample.

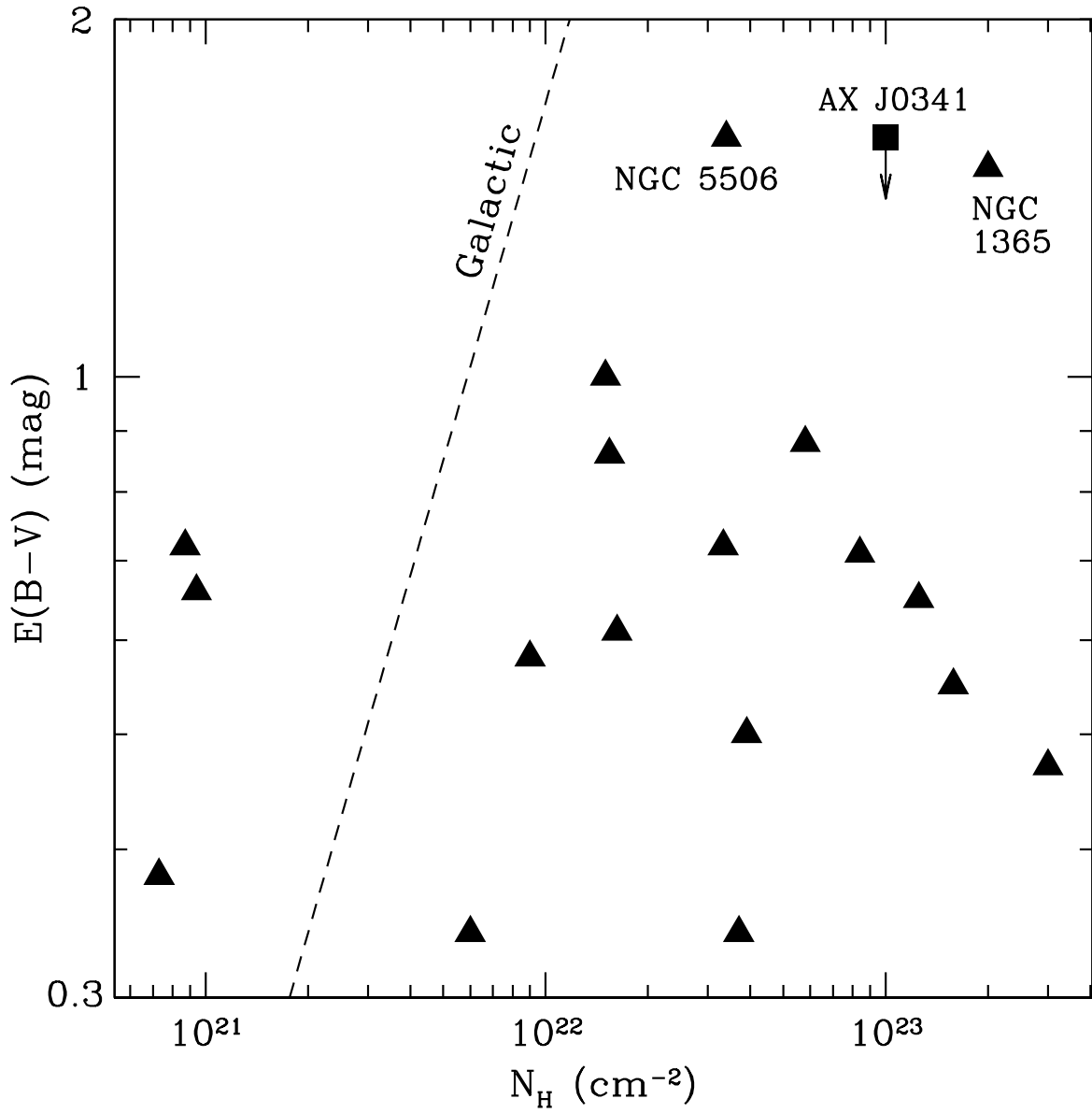


Fig. 2.— Reddening versus column density for the objects in the M01a sample. The box corresponds to AX J0341-44, for which only an upper limit has been established for the reddening. The dashed line is the average reddening for the diffuse ISM in our Galaxy.

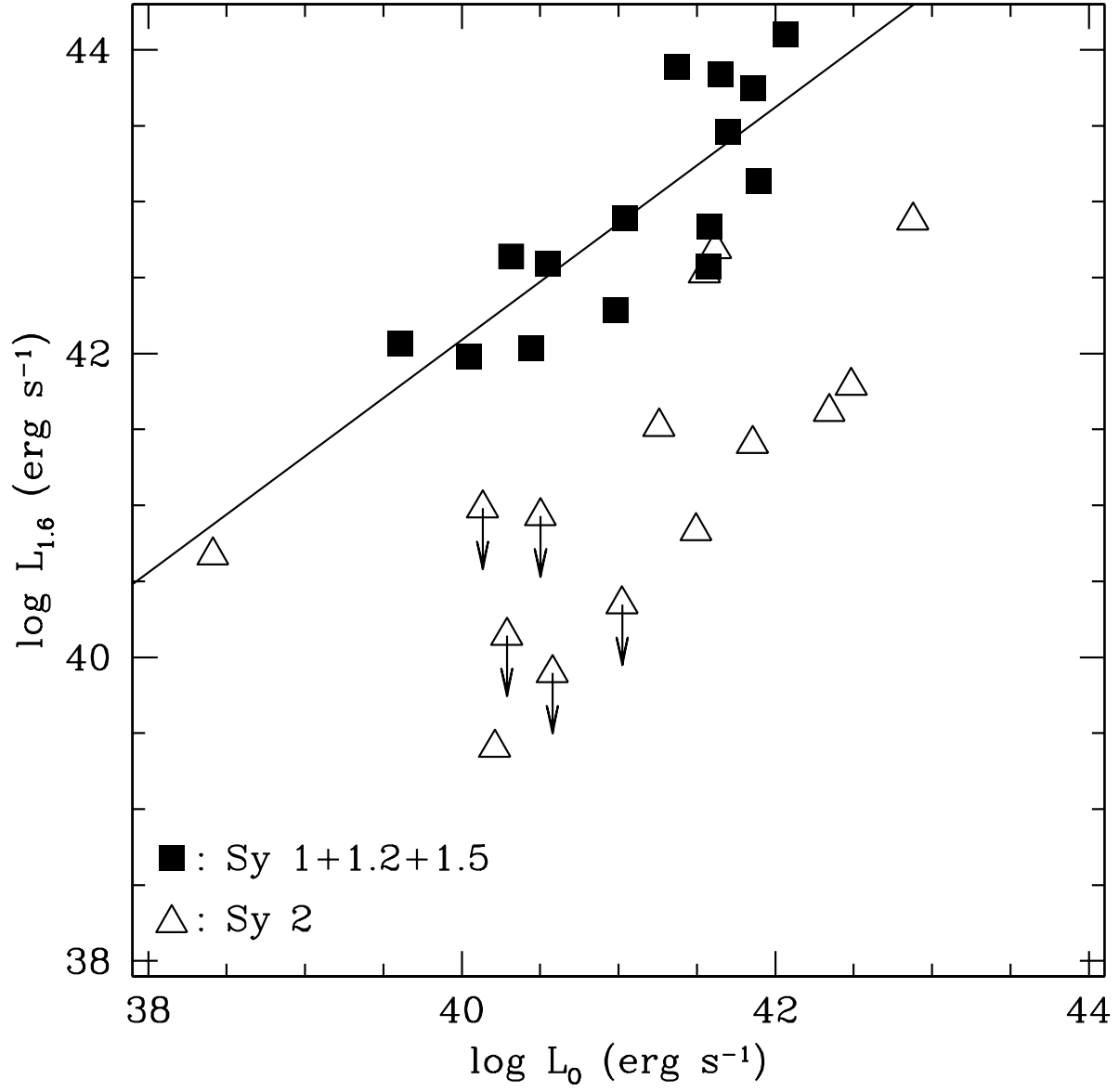


Fig. 3.— Luminosity at $1.6\mu\text{m}$ versus [O III] $\lambda 5007$ luminosity for Seyfert galaxies in Tables 2 and 3. The solid line is a least squares fit for Sy 1+1.2+1.5 galaxies. Arrows indicate upper limits.

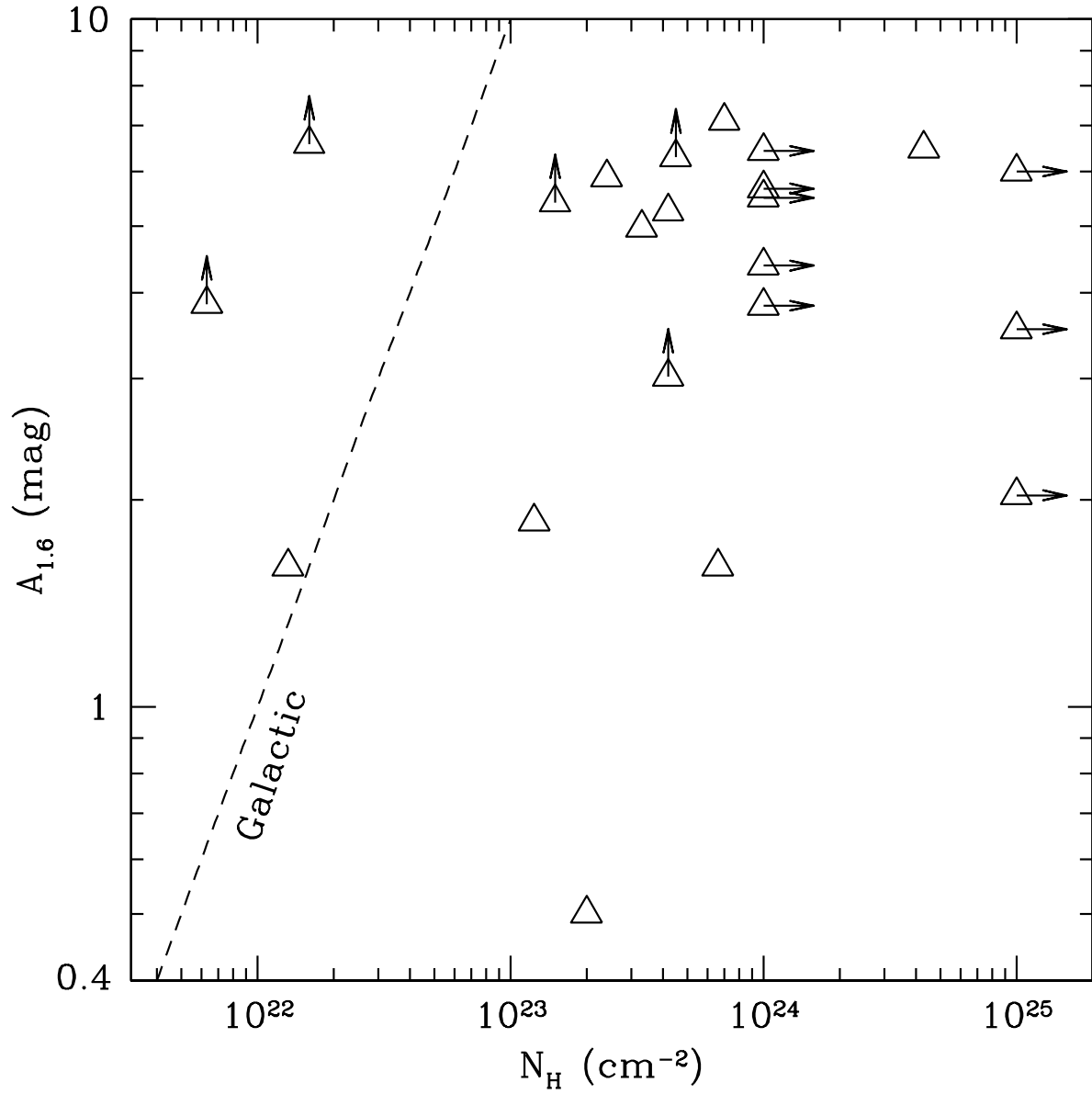


Fig. 4.— Inferred extinction at $1.6\mu\text{m}$ (see §4) versus column density for Sy 2s from Table 3. Arrows indicate lower limits. The dashed curve is the $1.6\mu\text{m}$ extinction for the diffuse ISM in our Galaxy.

Table 1. M01a Sample of AGNs

| Name | $E(B-V)$ mag | N_{H} 10^{20} cm^{-2} | $E(B-V)/N_{\mathrm{H}}$ rel. Gal. ^b | Type ^a |
|-----------------|-----------------|---|---|-------------------|
| M 81 | 0.66 | 9.4 | 4.11 | 1.8 |
| NGC 4639 | 0.38 | 7.3 | 3.04 | 1.8 |
| NGC 5033 | 0.72 | 8.7 | 4.84 | 1.9 |
| NGC 1365 | 1.5 | 2000 | 0.022 | 1.8 |
| Mrk 231 | 0.34 | 370 | 0.054 | 1 |
| IRAS 13197-1627 | 0.47 | 3000 | 0.0092 | 1.8 |
| SAX J1519+65 | 0.55 | 1580 | 0.020 | 1.9 |
| NGC 5506 | 1.59 | 340 | 0.27 | 1.9 |
| NGC 2992 | 0.58 | 90 | 0.38 | 1.9 |
| SAX J0045-25 | 0.5 | 390 | 0.075 | 1.9 |
| Mrk 6 | 0.72 | 333 | 0.13 | 1.5 |
| MCG-5-23-16 | 0.61 | 162 | 0.22 | 2 |
| SAX J1218+29 | 0.65 | 1250 | 0.030 | 1.9 |
| IRAS 05189-2524 | 0.71 | 840 | 0.049 | 2 |
| NGC 526a | 1.0 | 150 | 0.39 | 1.9 |
| 3C 445 | 0.88 | 580 | 0.088 | 1 |
| SAX J1353+18 | 0.86 | 154 | 0.33 | |
| AX J0341-44 | < 1.59 | 1000 | < 0.09 | |
| PG 2251+11 | 0.34 | 60 | 0.33 | |

^aSeyfert type, if available. From the NASA/IPAC Extragalactic Database (NED), with the following exceptions: SAX J1519+65, J0045-25, and J1218+29 (Maiolino et al. 2000); NGC 2992 (Gilli et al. 2000); NGC 526a (Landi et al. 2001).

^bObserved values of $E(B-V)/N_{\mathrm{H}}$ are given relative to the Galactic value of $E(B-V)/N_{\mathrm{H}} = 1.7 \times 10^{-22} \text{ mag cm}^2$. For comparison, the mean Galactic column density, for given latitude $|b| > 2^\circ.5$, is $N_{\mathrm{H}} = 2.9 \times 10^{20} \text{ csc } |b| \text{ cm}^{-2}$ (Dickey & Lockman 1990).

Table 2. Seyfert 1+1.2+1.5 Galaxies

| Name | [O III] flux ^a $10^{-11} \text{ erg s}^{-1} \text{ cm}^{-2}$ | $1.6\mu\text{m}$ flux ^b mJy | v_r ^c km s^{-1} |
|----------|--|---|--|
| NGC 3227 | 0.064 | 13.2 | 1145 |
| NGC 3516 | 0.048 | 18.1 | 2624 |
| NGC 4151 | 1.16 | 112.1 | 990 |
| NGC 4235 | 0.0024 | 3.69 | 2255 |
| NGC 4593 | 0.0172 | 10.1 | 2496 |
| NGC 5548 | 0.058 | 17.7 | 5100 |
| NGC 6814 | 0.0136 | 6.25 | 1563 |
| NGC 7469 | 0.058 | 48.3 | 4807 |
| Mrk 6 | 0.075 | 30.6 | 5400 |
| Mrk 40 | 0.0072 | 0.78 | 6327 |
| Mrk 42 | 0.0012 | 1.35 | 7200 |
| Mrk 372 | 0.013 | 0.69 | 9306 |
| Mrk 915 | 0.046 | 4.25 | 1769 |
| Mrk 1048 | 0.021 | 12.2 | 12934 |
| IC 4329A | 0.034 | 59.4 | 4574 |

^aFrom Whittle 1992

^bFrom Quillen et al. 2001

^cRadial velocity, from SIMBAD

Table 3. Seyfert 2 Galaxies

| Name | [O III] flux ^a 10 ⁻¹¹ erg s ⁻¹ cm ⁻² | 1.6 μ m flux ^b mJy | v_r ^c km s ⁻¹ | A _{1.6} mag | N_H ^a 10 ²⁰ cm ⁻² | $A_{1.6}/N_H$ rel. Gal. |
|----------------|---|--------------------------------------|--|-------------------------|---|----------------------------|
| NGC 3081 | 0.215 | 13.4 | 2413 | 1.60 | 6600. | 2.4E-2 |
| NGC 4388 | 0.374 | 0.71 | 2400 | 5.25 | 4200. | 1.2E-1 |
| NGC 5128 | 0.006 | 5.8 | 360 | 0.50 | 2000. | 2.4E-2 |
| NGC 5194 | 0.228 | 0.19 | 463 | 7.11 | 7000. | 9.9E-2 |
| NGC 7582 | 0.445 | 22.6 | 1545 | 1.86 | 1240. | 1.5E-1 |
| IC 5063 | 0.353 | 0.32 | 3402 | 5.89 | 2400. | 2.4E-1 |
| Circinus | 6.970 | 4.77 | 439 | 6.48 | 4.3E4 | 1.5E-2 |
| IRAS 1832-5926 | 0.752 | 22.7 | 6069 | 1.60 | 132. | 1.2 |
| NGC 7319 | 0.024 | 0.07 | 6611 | 4.97 | 3300. | 1.5E-1 |
| NGC 2639 | 0.004 | < 0.15 | 3198 | > 3.02 | 4200. | > 7.0E-2 |
| NGC 4258 | 0.262 | < 1. | 472 ^d | > 5.41 | 1500. | > 3.5E-1 |
| NGC 4941 | 0.355 | < 0.4 | 945 | > 6.30 | 4500. | > 1.4E-1 |
| NGC 1672 | 0.077 | < 1.1 | 1114 | > 3.85 | 63. | > 5.9 |
| NGC 3079 | 0.090 | < 0.1 | 1125 | > 6.58 | 160. | > 4.0 |
| NGC 1068 | 15.8 | 83.6 | 1200 | 3.54 | > 1.E5 | < 3.4E-3 |
| NGC 2273 | 0.277 | 0.32 | 1840 | 6.00 | > 1.E5 | < 5.8E-3 |
| NGC 5135 | 0.614 | 0.66 | 3866 | 5.50 | > 1.E4 | < 5.3E-2 |
| NGC 5347 | 0.100 | 0.97 | 2335 | 3.83 | > 1.E4 | < 3.7E-2 |
| Mrk 1066 | 0.513 | 0.51 | 3600 | 5.67 | > 1.E4 | < 5.5E-2 |
| NGC 7674 | 0.185 | 4.39 | 8766 | 2.03 | > 1.E5 | < 2.0E-3 |
| Mrk 1210 | 0.482 | 1.51 | 4049 | 4.38 | > 1.E4 | < 4.2E-2 |
| Mrk 477 | 1.238 | 0.29 | 11318 | 6.43 | > 1.E4 | < 6.2E-2 |

^aFrom Bassani et al. 1999 and Risaliti et al. 1999

^bFrom Quillen et al. 2001

^cRadial velocity, from SIMBAD

^dFrom Cecil et al. 1992